Fabrication-Friendly Random Meta-Atom Generation for Phase-Shifting Metasurfaces

Haiyang Huang, Xiaojie Zhang, Fuwan Gan, and Xingjie Ni

***Abstract*—Compared with traditional phase-shifting metasurface design methods, computer-aided optimization has attracted significant interest due to its advantages of high efficiency and a wide modulation range, resulting in the ability to generate various random-shaped meta-atoms to maximize their phase modulation capabilities. However, these meta-atoms often have sharp boundaries, chamfers, microscopic particles, and small holes, which are unsuitable for micro-/nano-fabrication. We propose a method to generate 2D meta-balls, which can generate random-shaped meta-atoms with smooth boundaries free of small particles or holes and suitable for micro-/nano-fabrication. This method can easily control the characteristics of generated shapes, such as boundary continuity and symmetry. It is simple, straightforward, and time-saving, and it helps in computer-aided optimization phase-shifting metasurfaces design.**

***Index Terms*—Fabrication-friendly, random meta-atom generation, computer-aided optimization, metasurfaces.**

I. Introduction

METASURFACES have attracted broad interest due to their potential in photonic applications. A conventional process to construct a metasurface is first to create a meta-atom library [1], [2]. These meta-atoms are a collection of sub-wavelength-sized geometric shapes with different optical responses. Those meta-atoms are arranged in a lattice to form the metasurface. Early metasurfaces were based on regular-shaped meta-atoms, such as rectangular parallelepipeds, cylinders, concentric rings, and L-shaped structures, which have only a few adjustable parameters [3]–[6]. Such designs are driven by human intuition and limited by designer experience. The designing process is inefficient. Unlike conventional methods, computer-aided optimization methods can achieve various random-shaped meta-atoms that cannot be designed manually, provide a large meta-atom library, and augment performance [7]–[14]. Research has demonstrated various optical devices based on computer-aided optimization, such as wavelength demultiplexer[15], particle accelerator [16], achromatic metalenses [17], [18], and etc.

There are many ways to generate random-shaped meta-atoms [19]–[22], but the generated meta-atoms may have sharp chamfers or shapes that are too small isolated islands or holes, which are challenging to fabricate. Some methods can generate fabrication-friendly shapes, but they involve additional analysis and optimization, which is time- and energy-consuming. Here, we propose a meta-balls-based algorithm that can quickly generate an extensive and easy-to-fabricate meta-atom shape library for construcing functional metasurfaces. The generated shapes are random and boundary-smooth with controllable characteristics, such as boundary continuity and symmetry, which facilitates the design of polarization-independent metasurfaces.

II. Methods

Our method is based on two-dimensional meta-balls. It was proposed by Jim Blinn in 1982 and is referred to colloquially as the "jelly effect" [23]. Meta-balls are implicit surfaces, which are not clearly defined by vertices (such as meshes) or control points (such as surfaces). Their shape and form are controlled by mathematical formulas. The creation of multiple spheres allows the values to interact, causing them to change shape and blend with surrounding deformed spheres when they are close together. The process creates effectively smooth surfaces. Meta-balls are usually used to create isosurfaces in 3D space. When designing metasurfaces, we only need to use 2D meta-balls to create planar contours. The generation function is not unique. In theory, any continuous function can yield a random surface. Inverse square and Gaussian functions are commonly used. We used an inverse square function below, where the contribution of the terms to the function gradually decreases with increasing distance from the centers of the circles.

$$f(x,y)=\sum_{i=0}^{n}\frac{r_i^2}{(x-x_i)^2+(y-y_i)^2}$$

where n is the number of circles, and r_i and (x_i, y_i) are the radius and center, respectively, of circle i.

Next, we use the level set method to define the boundary of the meta-atoms. The level set method was first proposed by Osher and Sethian [24] in 1988, and has been successfully applied

Manuscript received November 19, 2021; accepted January 16, 2022. Date of publication January 21, 2022; date of current version January 31, 2022. This work was supported in part by the National Key Research and Development Program of China under Grant 2017YFA0206403, in part by the Science and Technology Commission of Shanghai Municipality under Grant 16ZR1442600, in part by the Shanghai Municipal Science and Technology Major Project under Grant 2017SHZDZX03, and in part by the National Natural Science Foundation of China under Grants 92163134, 62075232, and 62005305. *(Corresponding author: Fuwan Gan.)*

Haiyang Huang and Fuwan Gan are with the State Key Laboratory of Functional Materials for Informatics, Shanghai Institute of Microsystem and Information Technology, Chinese Academy of Sciences, Shanghai 200050, China, and also with the University of Chinese Academy of Sciences, Beijing 100049, China (e-mail: huanghy@mail.sim.ac.cn; fuwan@mail.sim.ac.cn).

Xiaojie Zhang and Xingjie Ni are with the Department of Electrical Engineering, The Pennsylvania State University, University Park, PA 16802 USA, and also with the Materials Research Institute, The Pennsylvania State University, University Park, PA 16802 USA (e-mail: xxz321@psu.edu; xingjie@psu.edu).

Digital Object Identifier 10.1109/JPHOT.2022.3144434

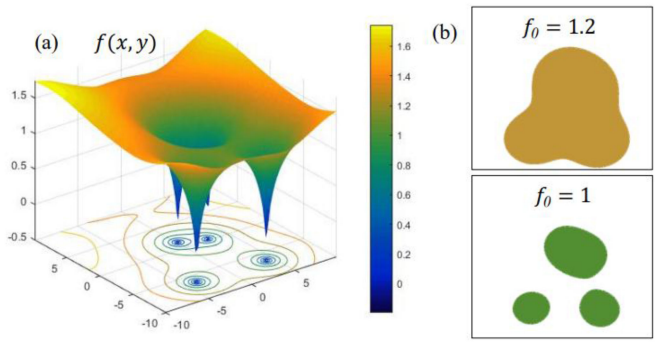

Fig. 1. (a) Three-dimensional function image of $f(x, y)$ and the corresponding contours. A contour is formed by letting $f\ (x, y) = f_0$. Contour colors correspond to different values of f_0; (b) A meta-atom with a smooth boundary is obtained with level set method: selecting a contour value f_0 and filling its enclosed area.

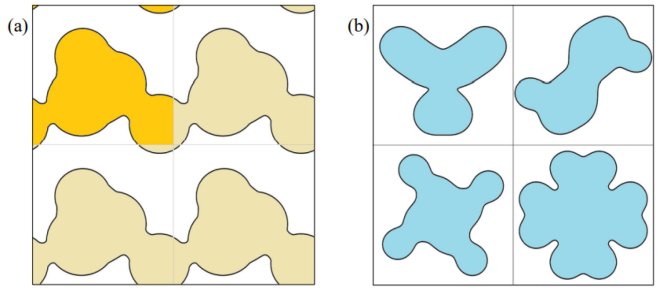

Fig. 2. (a) Meta-atoms with continuous boundaries in x and y directions; (b) meta-atoms with axisymmetry, centrosymmetry, order 4 rotational symmetry, and four-fold reflection symmetry, respectively.

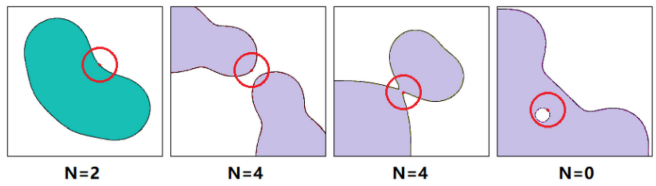

Fig. 3. The circle's center (red), with its radius fixed to the minimum fabricable dimension δ, travels along a contour. The number of intersections between the circle and contour is N. (a) N = 2: the shape can be fabricated; (b) N = 4: the local gap is too small to be fabricated; (c) N = 4: the local shape is too narrow to be fabricated; (d) N = 0: the shape cannot be fabricated because of the presence of holes that are too small.

in computer graphics segmentation and topology optimization [25]–[29]. The basic idea of the level set method level set method is to define a one dimension higher surface and use the zero level set of the function to represent the boundary of an object and control the evolution of the boundary by updating the level set surface. Here, by letting $f\ (x, y) = f_0$ in the function value domain, the corresponding boundary contour in the *x*–*y* plane can be obtained, as shown in Fig. 1a. The contours generally are smooth closed curves of one or more segments, dividing the plane into several regions. We assign the areas of $f \geq f_0$ and $f < f_0$ to 1 and 0, respectively. We fill areas assigned to 1 with metasurface material and etch areas assigned to 0. We use the MATLAB contour function to obtain the contours and fill in each area numerically to form random-shaped meta-atoms, as shown in Fig. 1b.

To meet metasurfaces' design and fabrication requirements, we need to optimize the shape of a random-shaped meta-atom further. Shapes generated by the meta-balls method may be discontinuous due to truncation at the boundaries between adjacent unit cells, which may cause problems when shapes are imported into an electromagnetic model with Bloch boundaries. A practical solution is to expand the unit cell to a 3×3 area and copy the function $f(x, y)$ to the surrounding eight sub-unit cells. Denoting the side lengths of a unit cell by a and b, the function replicated with translations is expressed by

$$\begin{aligned} f_{periodic}\ (x, y) \ = \ & f\ (x, y) + f\ (x + a, y) + f\ (x - a, y) \\ & + f\ (x, y + b) + f\ (x, y - b) \\ & + f\ (x + a, y + b) + f\ (x + a, y - b) \\ & + f\ (x - a, y - b) + f\ (x - a, y + b) \end{aligned}$$

With the above function, the contours at the central unit cell boundary are fused and periodic in the x and y directions, as shown in Fig. 2a. It ensures that the boundaries of adjacent unit cells are smooth and continuous. To strictly follow the periodicity, an appropriate $f\ (x, y) = f_0$ must be selected so that the span of each contour in the x and y directions is less than [2a, 2b]. It ensures that $f(x, y)$ of the central unit cell is only affected by the eight nearest sub-unit cell neighbors, and sampling at greater distances is ignored.

Polarization is another property that could be considered in metasurfaces design [30]. A meta-atom design often uses symmetric shapes, which can introduce polarization-independent characteristics to metasurfaces. Similar to periodic expansion, symmetry only requires corresponding symmetric operations on the function $f(x, y)$ and their superimposition. For example, For meta-atoms shapes with fourfold reflection symmetry, the function can be rewritten as

$$\begin{aligned} f_{four-fold}\ (x, y) \ = \ & f\ (x, y) + f\ (-y, x) + f\ (-x, -y) \\ & + f\ (y, -x) + f\ (y, x) + f\ (-x, y) \\ & + f\ (-y, -x) + f\ (x, -y) \end{aligned}$$

where $f(y, x)$ is the axial symmetry term of $f(x, y)$ about $y = x$, and the first four terms and last four terms of the formula are 90° rotational symmetry items of $f(x, y)$ and $f(y, x)$ about the center. After these symmetry operations, the shape of fourfold reflection symmetry can be obtained, as shown in Fig. 2b.

Micro-/nano-fabrication has a minimum line width δ, and a smaller shape cannot be fabricated accurately. We use post-screening to eliminate these shapes, as shown in Fig. 3, where O is a point on contour line A. The function values on the two sides of the contour line are $f = 0$ and $f\ = \ 1$. For a circle C with center O and radius δ, we count the number of times N that f changes between 0 and 1 while traversing the circumference of circle C. Fabricable shapes meet the requirement that the minimum line width is greater than δ, so there are only two intersection points between circle C and contour S, where f transitions from 0 to 1 and 1 to 0, so N = 2 (Fig. 3a). If the

minimum line width of the shape is less than δ, then N will not equal 2 at some points on the contour. As shown in Fig. 3b and c, sufficiently small spacing between generated shapes or narrow areas of shapes can result in N greater than 2. In addition, as shown in Fig. 3d, when the generated shape is a small, isolated pixel or hole, then $N < 2$. Fabricable shapes must be detected at point A on the contour and must satisfy $N = 2$; otherwise, they are removed.

It should be mentioned that for periodically constructed shapes, the detection ranges of contours in the x and y directions should be $[-a/2-\delta, a/2+\delta]$ and $[-b/2-\delta, b/2+\delta]$, respectively, to avoid possible detection errors at the unit cell boundaries. In MATLAB, the contour curve obtained by the contour function is a polyline. The smaller the length l of a line segment in the polyline, and the smaller the minimum step length s around circle C, the more accurate the estimation result, but more calculation is required. We set the length of each segment l and the minimum step size s to $l = \delta/4$ and $s = \delta/12$, respectively, for a good tradeoff between accuracy and the calculation complicity.

Based on the above shape optimization and screening schemes, we demonstrate a metasurface based on random smooth shapes and achieve beam steering functionality. Each meta-atom design is a reverse design based on surrogate optimization [31], [32], which is based on random search approach. Surrogate optimization tries to find the global minimum of the objective function using few objective function evaluations without requiring a good initial value or gradient information. It minimizes the times of the computationally expensive full-wave evaluations. According to the principle of meta-balls method, meta-atoms are represented by the union of a set of circles with different radii and center positions. Their initial shape is cylindrical, located in the center of the unit cell. The optimizer calculates the cost function value with a full-wave-simulation-based evaluator, which extracts both the spectroscopic phase and diffraction efficiency for the input shape. If the cost function value is smaller than a predefined number, the process stops, and the current optimal shape is output. Otherwise, the optimizer invokes the shape generation process, where the shape generator creates a set of distorted shapes through randomly changing the parameters (numbers, radii, and positions of circles) in the meta-balls generation function. It is worth noting that we adapted the surrogate algorithm to reduce the invocation times for the evaluator. Instead of directly calling the evaluator function to get full wave simulation, we used a radial basis interpolation to estimate the value of the cost function. Only the shape with lowest estimated cost function value would be evaluated by the evaluator. If the cost function value is reduced, the algorithm updates the record of the current optimal shape.

The optimized result is shown in Fig. 4a. This super unit cell of the metasurface consists of four meta-atoms with smooth boundaries and phase modulation of 0, $\pi/2$, π, and $3\pi/2$, respectively. The simulated field distribution is shown in Fig. 4b. A 1550-nm plane wave is an incident from the SiO_2 substrate (left in the figure), and 45° beam steering is achieved after passing through the metasurface. It should be mentioned that the metasurface is not polarization independent, because the period difference in x and y direction breaks the symmetry. The simulation

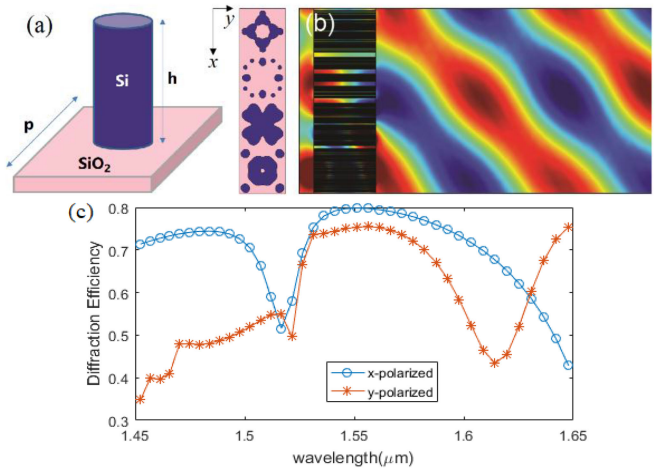

Fig. 4. (a) Schematic diagram of a 3D meta-atom model. The meta-atom of Si material is built on the SiO_2 substrate. Their refractive indices are 3.45 and 1.5. The height of the meta-atom is h = 800 nm. The period of the unit cell is p = 600 nm. Four kinds of meta-atoms with smooth boundaries can achieve phase modulations of 0, $\pi/2$, π, and $3\pi/2$, forming a super unit cell; (b) Electric field distribution from 3D full-wave electromagnetic simulations. An x-polarized plane wave with a wavelength of 1550 nm is incident from the substrate (left side). It undergoes phase modulation when passing through the metasurface, achieving beam steering with the deflection angle at about 45°. (c) The diffraction efficiency values for x-polarized and y-polarized incident light and their wavelength dependence.

results show that the diffraction efficiency for x-polarized and y-polarized incident light at 1550 nm wavelength are 79.8% and 75.5%, respectively. Both wavelength dependences are shown in Fig. 4c. We could further optimize the structure to achieve better performance, such as a larger bandwidth.

III. Conclusion

In summary, we have proposed a new method to generate fabrication-friendly random-shaped meta-atoms for metasurfaces. This method generates random and smooth 2D meta-balls and then obtains a random-shaped meta-atom. Applying the method to metasurfaces, we carried out boundary continuity optimization, symmetry optimization, and minimum linewidth screening. We used a computer-aided optimization algorithm to demonstrate a beam steering metasurface based on random smooth shapes. With its advantages of simplicity and speed, and the ability to build an extensive resource library, this method has good application potential in computer-aided optimization of metasurface with random shaped meta-atom designs.

References

[1] S. Molesky *et al.*, "Inverse design in nanophotonics," *Nature Photon.*, vol. 12, no. 11, pp. 659–670, 2018.
[2] E. B. Whiting *et al.*, "Meta-atom library generation via an efficient multi-objective shape optimization method," *Opt. Exp.*, vol. 28, no. 16, pp. 24229–24242, 2020.
[3] S. Wang *et al.*, "A broadband achromatic metalens in the visible," *Nature Nanotechnol.*, vol. 13, no. 3, pp. 227–232, 2018.
[4] W. T. Chen *et al.*, "A broadband achromatic metalens for focusing and imaging in the visible," *Nature Nanotechnol.*, vol. 13, no. 3, pp. 220–226. 2018.
[5] H. Zhou *et al.*, "Broadband achromatic metalens in the midinfrared range," *Phys. Rev. Appl.*, vol. 11, no. 2, 2019, Art. no. 024066.

[6] E. Arbabi *et al.*, "Multiwavelength polarization-insensitive lenses based on dielectric metasurfaces with meta-molecules," *Optica*, vol. 3, no. 6, pp. 628–633, 2016.

[7] N. Lebbe *et al.*, "Robust shape and topology optimization of nanophotonic devices using the level set method," *J. Comput. Phys.*, vol. 395, pp. 710–746, 2019.

[8] E. W. Wang *et al.*, "Robust design of topology-optimized metasurfaces," *Opt. Mater. Exp.*, vol. 9, no. 2, pp. 469–482, 2019.

[9] S. An *et al.*, "Multifunctional metasurface design with a generative adversarial network," *Adv. Opt. Mater.*, vol. 9, no. 5, 2021, Art. no. 2001433.

[10] T. Phan *et al.*, "High-efficiency, large-area, topology-optimized metasurfaces," *Light: Sci. Appl.*, vol. 8, no. 1, pp. 1–9, 2019.

[11] J. Rong and W. Ye, "Multifunctional elastic metasurface design with topology optimization," *Acta Materialia*, vol. 185, pp. 382–399, 2020.

[12] Z. A. Kudyshev *et al.*, "Machine-learning-assisted metasurface design for high-efficiency thermal emitter optimization," *Appl. Phys. Rev.*, vol. 7, no. 2, 2020, Art. no. 021407.

[13] Z. Lin and S. G. Johnson, "Overlapping domains for topology optimization of large-area metasurfaces," *Opt. Exp.*, vol. 27, no. 22, pp. 32445–32453, 2019.

[14] R. Pestourie *et al.*, "Inverse design of large-area metasurfaces," *Opt. Exp.*, vol. 26, no. 26, pp. 33732–33747, 2018.

[15] A. Y. Piggott *et al.*, "Inverse design and demonstration of a compact and broadband on-chip wavelength demultiplexer," *Nature Photon.*, vol. 9, no. 6, pp. 374–377, 2015.

[16] N. V. Sapra *et al.*, "On-chip integrated laser-driven particle accelerator," *Science*, vol. 367, no. 6473, pp. 79–83, 2020.

[17] Y. Zhou *et al.*, "Multilayer noninteracting dielectric metasurfaces for multiwavelength metaoptics," *Nano Lett.*, vol. 18, no. 12, pp. 7529–7537, 2018.

[18] X. Zhang *et al.*, "Broadband polarization-independent achromatic metalenses with unintuitively-designed random-shaped meta-atoms," 2021, *arXiv:2103.10845*.

[19] S. Shrestha *et al.*, "Broadband achromatic dielectric metalenses," *Light: Sci. Appl.*, vol. 7, no. 1, pp. 1–11, 2018.

[20] Z.-B. Fan *et al.*, "A broadband achromatic metalens array for integral imaging in the visible," *Light: Sci. Appl.*, vol. 8, no. 1, pp. 1–10, 2019.

[21] J. Rho and J. A. Fan, "Freeform metasurface design based on topology optimization," *MRS Bull.*, vol. 45, no. 3, pp. 196–201, 2020.

[22] W. Kong *et al.*, "Bidirectional cascaded deep neural networks with a pretrained autoencoder for dielectric metasurfaces," *Photon. Res.*, vol. 9, no. 8, pp. 1607–1615, 2021.

[23] J. F. Blinn, "A generalization of algebraic surface drawing," *ACM Trans. Graph.*, vol. 1, no. 3, pp. 235–256, 1982.

[24] S. Osher and J. A. Sethian, "Fronts propagating with curvature-dependent speed: Algorithms based on Hamilton-Jacobi formulations," *J. Comput. Phys.*, vol. 79, no. 1, pp. 12–49, 1988.

[25] M. Mansouree and A. Arbabi, "Metasurface design using level-set and gradient descent optimization techniques," in *Proc. IEEE Int. Appl. Comput. Electromagnetics Soc. Symp.*, 2019, pp. 1/2.

[26] Y. Noguchi and T. Yamada, "Level set-based topology optimization for graded acoustic metasurfaces using two-scale homogenization," *Finite Elements Anal. Des.*, vol. 196, 2021, Art. no. 103606.

[27] K. Miyata *et al.*, "Optimum design of a multi-functional acoustic metasurface using topology optimization based on Zwicker's loudness model," *Comput. Methods Appl. Mechanics Eng.*, vol. 331, pp. 116–137, 2018.

[28] P. Vogiatzis *et al.*, "Computational design and additive manufacturing of periodic conformal metasurfaces by synthesizing topology optimization with conformal mapping," *Comput. Methods Appl. Mechanics Eng.*, vol. 328, pp. 477–497, 2018.

[29] M. Y. Shalaginov *et al.*, "Design for quality: Reconfigurable flat optics based on active metasurfaces," *Nanophotonics*, vol. 9, no. 11, pp. 3505–3534, 2020.

[30] S. Wang *et al.*, "Arbitrary polarization conversion dichroism metasurfaces for all-in-one full Poincaré sphere polarizers," *Light: Sci. Appl.*, vol. 10, no. 1, pp. 1–9, 2021.

[31] N. V. Queipo *et al.*, "Surrogate-based analysis and optimization," *Prog. Aerosp. Sci.*, vol. 41, no. 1, pp. 1–28, 2005.

[32] H.-M. Gutmann, "A radial basis function method for global optimization," *J. Glob. Optim.*, vol. 19, no. 3, pp. 201–227, 2001.